LBL--29783

DE91 004125

OSSY Source Characterization—Summary Report

L. R. Johnson and T. V. McEvilly

Earth Sciences Division
Lawrence Berkeley Laboratory
University of California
Berkeley, California 94720

September 1990

This work was done at Lawrence Berkeley Laboratory under the auspices of the U.S. Department of Energy Lawrence Livermore Laboratory under Contract No. W-7405-ENG-48. Data processing was done at the Lawrence Berkeley Laboratory Center for Computational Seismology under U.S. Department of Energy Contract No. DE-AC03-76SF00098.

Introduction

The On Site Seismic Yield (OSSY) experiment was performed during September 1989. It was a collaborative effort between scientists at the Lawrence Livermore National Laboratory, Lawrence Berkeley Laboratory, and the Seismographic Stations at UC Berkeley. It was performed in Yucca Valley at the Nevada Test Site (NTS).

The general objective of the OSSY experiment was to investigate techniques for using seismic measurements to estimate the yield of nuclear explosions. The basic idea is to use chemical explosions of known size to calibrate source coupling and wave propagation effects near the site of a nuclear explosion. Once calibrated in this way, seismic measurements, obtained at locations sufficiently far from the source to be in the region of linear elastic response but sufficiently close to provide accurate registration, can be used to estimate the yield of the nuclear explosion. If such a technique can be shown to be sufficiently accurate, it has the advantages of being relatively inexpensive, flexible in experimental design, and applicable to either large or small yields.

This investigation has proceeded in a two-stage process. The first stage is to develop and test the calibration procedure. The second stage is to apply the method to actual nuclear explosions. Partly because it was considered desirable to perform a complete analysis of the calibration procedure before applying it to a nuclear explosion and partly because no convenient nuclear explosion tests were available at the time, the OSSY experiment was concentrated on the calibration stage of the process.

The complete test of a technique such as this involves not only a demonstration that the method yields results of sufficient accuracy in specific applications, but also a development of the underlying physical principles to the point that it is possible to predict how the method will perform in a wide range of different applications. This second task requires a fairly basic understanding of the physics of an explosive source. In particular, knowledge must be available concerning the manner in which source size, source depth and source medium affect the elastic waves generated by explosive sources. This explains the comprehensive nature of the OSSY experiment, in that it had to be designed in such a way that information about each of these various aspects of the problem could be isolated in the data analysis stage. As a result, the experiment had several specific objectives which had to be accomplished in order to achieve the general objective.

One specific objective of this experiment was to investigate the effect of source depth upon the coupling of an explosive source. This was achieved by detonating a series of explosions at different depths in the same hole. Another objective was to check conventional scaling relationships for source size. This was achieved by varying the size of the explosions detonated in the hole. A third objective was to attempt to isolate the effect of source medium upon the coupling of an explosive source. This question was approached by conducting a special study of material properties in the vicinity of the hole before the detonation of the explosions. Another objective was to determine the accuracy of source properties which have been inferred from seismic observations made on the surface of the earth. This objective was achieved by making free-field measurements of motion in the hole near the source.

While the OSSY experiment did not include measurements of a buried nuclear explosion, it did include numerous measurements from buried chemical explosions. Furthermore, the investigations of source size, source depth, and source medium were carried out using chemical explosions with the idea of applying the results to nuclear explosions. It is clear that an important aspect of the basic approach being investigated here is to know if there are any fundamental differences in the way that elastic waves are generated by nuclear explosions and by chemical explosions. Thus a final objective was to determine if results obtained with chemical explosions of this type could be meaningfully compared with similar results for nuclear explosions.

The basic components of the experiment which are discussed in the present report include the following:

- A drilled hole bottoming in basement rocks at a depth of 658 meters
- Lithologic, velocity, and density logs of the hole
- A nine-component VSP survey of the hole and surrounding region
- A series of 24 explosions detonated in the hole at depths between 100 and 578 meters
- Free-field measurements of accelerations recorded within the hole at a range of distances from the explosions
- Surface measurements of ground motions caused by the explosions at locations which reversed the positions occupied by the sources in the VSP survey

It is worth noting that there were several other associated experiments performed by scientists from Lawrence Livermore National Laboratory, such as tests of an air-gun source and imaging of explosion cavities, but these will not be discussed in the present report.

In this first test of the calibration stage of the process it was considered important to explore the entire feasible range of the various design parameters that are involved in such an experiment. Thus, for instance, seismic measurements were made out to the maximum distance that useful information could conceivably be obtained. In addition, a considerable amount of redundancy was designed into the experiment. For these reasons, the OSSY experiment produced a large volume of data. It is expected

that because of the experience and information gained in this experiment, future experiments could be designed much more efficiently in terms of the data collection procedures, the data volume, and the data analysis procedures.

Experiment

The experiment was performed in the time period September 15 - 22, 1989. The experiment made use of a drilled hole, UE10ITS-3, in the northeastern end of Yucca Valley. The map in Figure 1 shows the location of the hole in Area 10 of NTS. An enlarged map is shown in Figure 2 which indicates the proximity of this hole to inferred faults in the area and also to other drilled holes in the area. Figures 3 and 4 present two geologic cross-sections through this area which have made use of the drill logs from the various holes. These sections are sufficient to determine the approximate thickness of the alluvium, the positions of three different tuff members of the sedimentary section, and the shape of the Paleozoic basement in the vicinity of hole UE10ITS-3. The hole was 658 meters deep, with the bottom extending 7 meters into Paleozoic basement rocks, which in this location are overlain by about 400 meters of tuff and 230 meters of alluvium (see Figure 3).

Prior to this experiment, the hole had been logged for both sonic velocity and density. In addition, before detonating the explosions, a complete nine-component VSP survey was conducted in the hole in order to characterize the velocities in the surrounding material. A three-component receiver was clamped in the hole at 35 different depths ranging over the depth interval of about 150 to 600 meters (Figure 5). For each of these depths, controlled three-component sources were placed at each of the ten receiver sites shown in Figure 5, which were along lines radiating from the hole in four different directions with offsets between 0 and 1200 meters. One of the primary purposes of the VSP survey was to calibrate wave propagation effects along source-receiver paths which were to be used later in the explosion part of the experiment. A by-product of the survey was fairly detailed velocity models for both P and S waves which could be used in the interpretation of the explosion data. In addition, the VSP survey was used to investigate possible seismic anisotropy in the area, to detect any strong velocity heterogeneity near the hole, and to measure attenuation properties.

After completing the VSP survey twenty four separate chemical explosions were detonated in this hole, with the deepest at a depth of 578 meters and the shallowest at 110 meters. The sizes of the explosions alternated between 10 and 100 pounds. Explosion parameters such as time, depth, and size are listed in Table 1. The details of how the explosions were emplaced and fired are contained in the report by Schaffer (1989).

The explosions were recorded by two surface networks of seismic stations deployed along lines radiating from the drilled hole at four different azimuths, with the maximum range being 1200 meters. Lawrence Livermore Laboratory deployed a network of vertical- component sensors and Berkeley deployed a network of three-component sensors. This Berkeley network produced usable data at 10 different stations at horizontal distances of between 22 and 626 meters of the hole. The

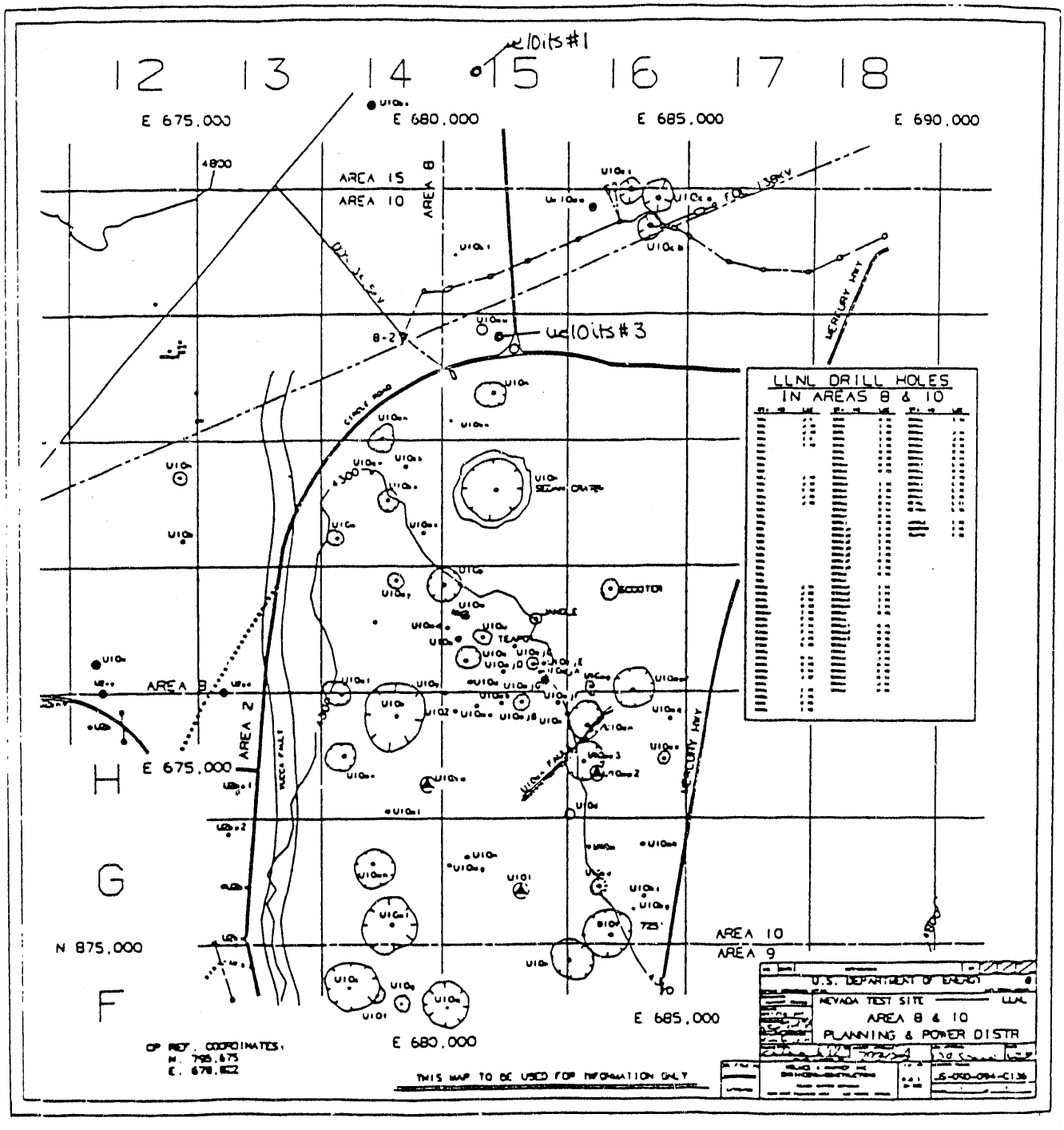

Figure 1. Map of areas 8 and 10 in the northeast corner of Yucca Valley at the Nevada Test Site.

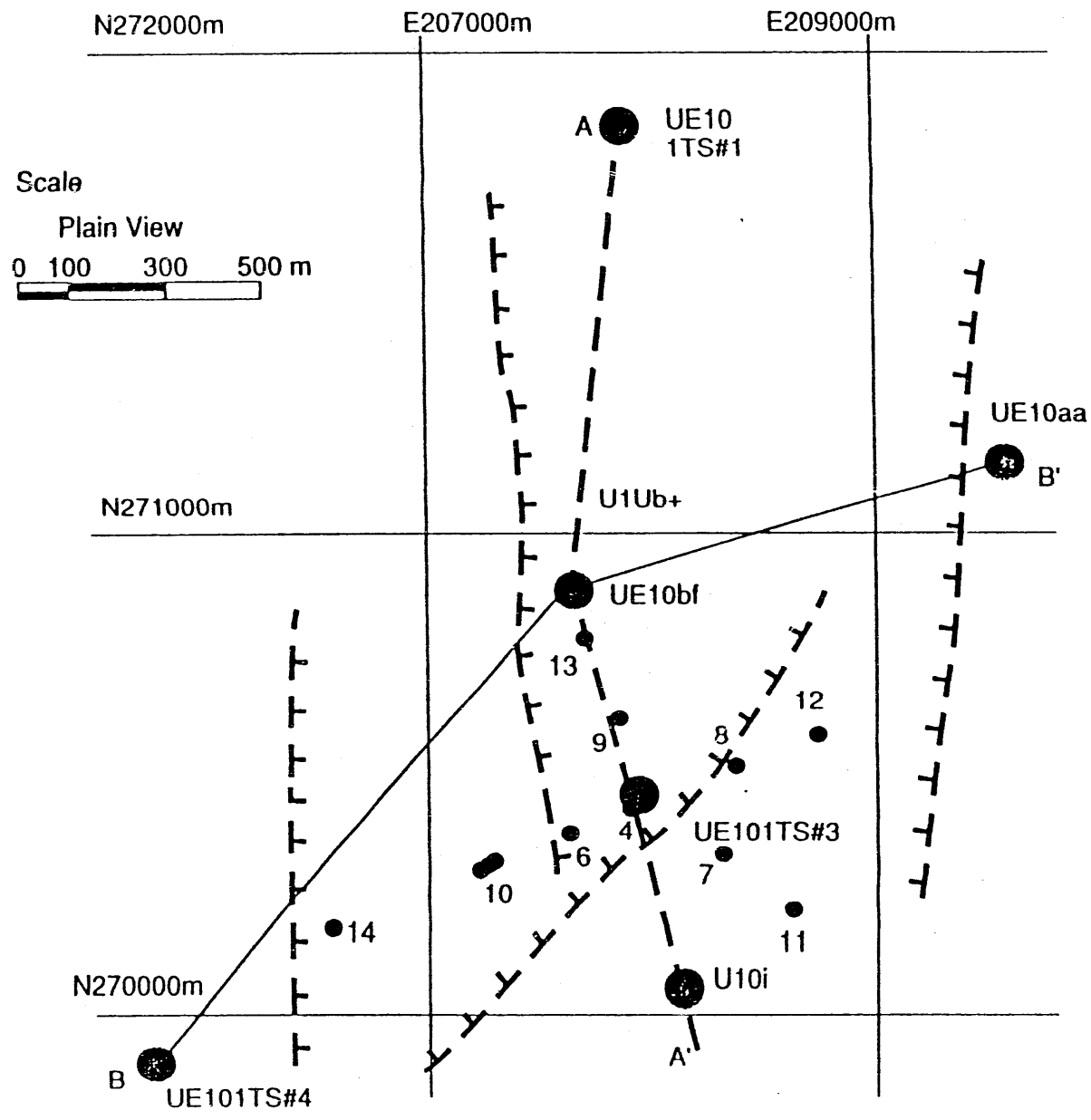

Figure 2. Enlarged map of the area near hole UE10ITS3. The lines AA' and BB' denote the locations of cross-sections shown in Figures 3 and 4, respectively.

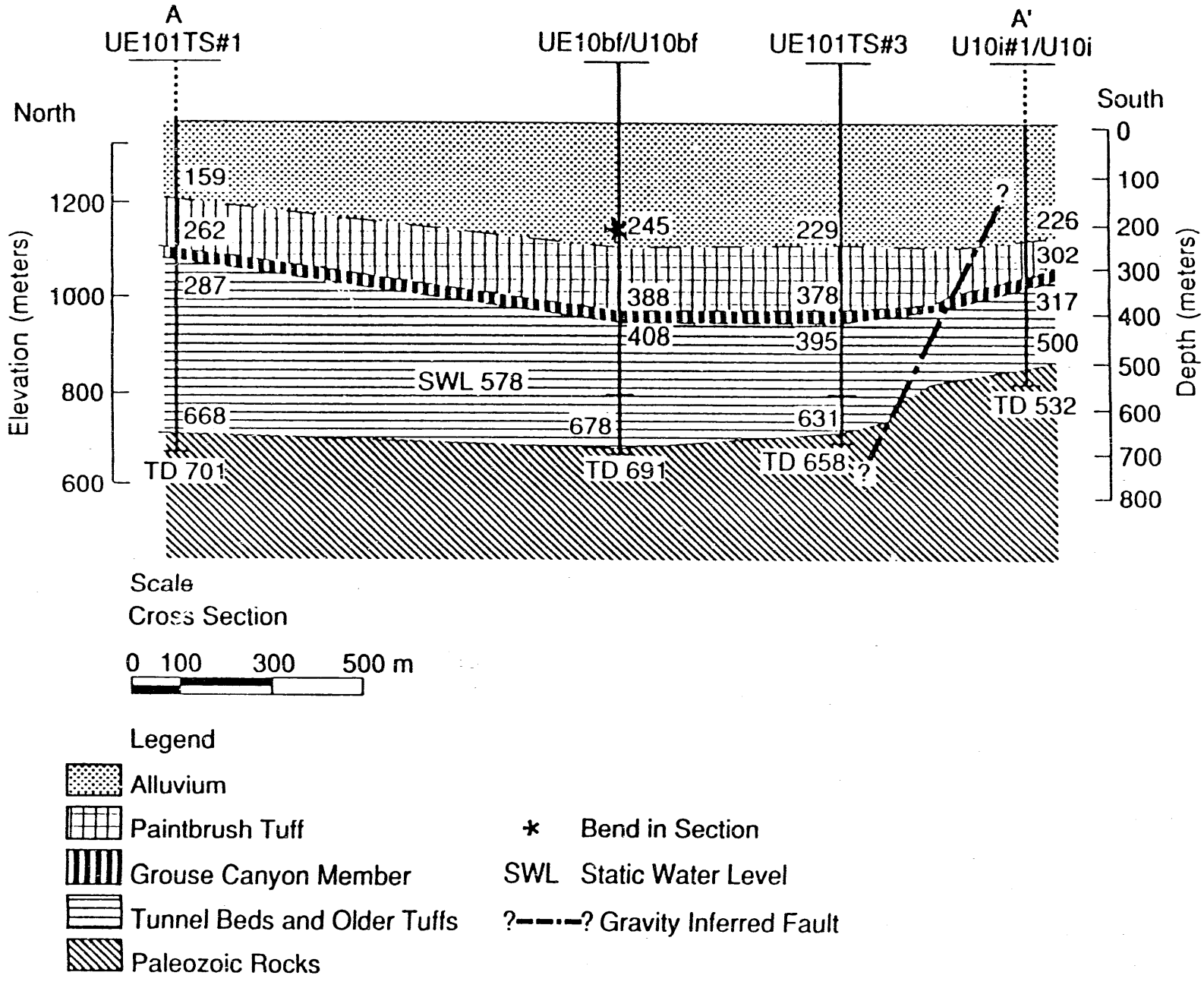

Figure 3. Geologic cross-section along the line AA' shown on the map of Figure 2.

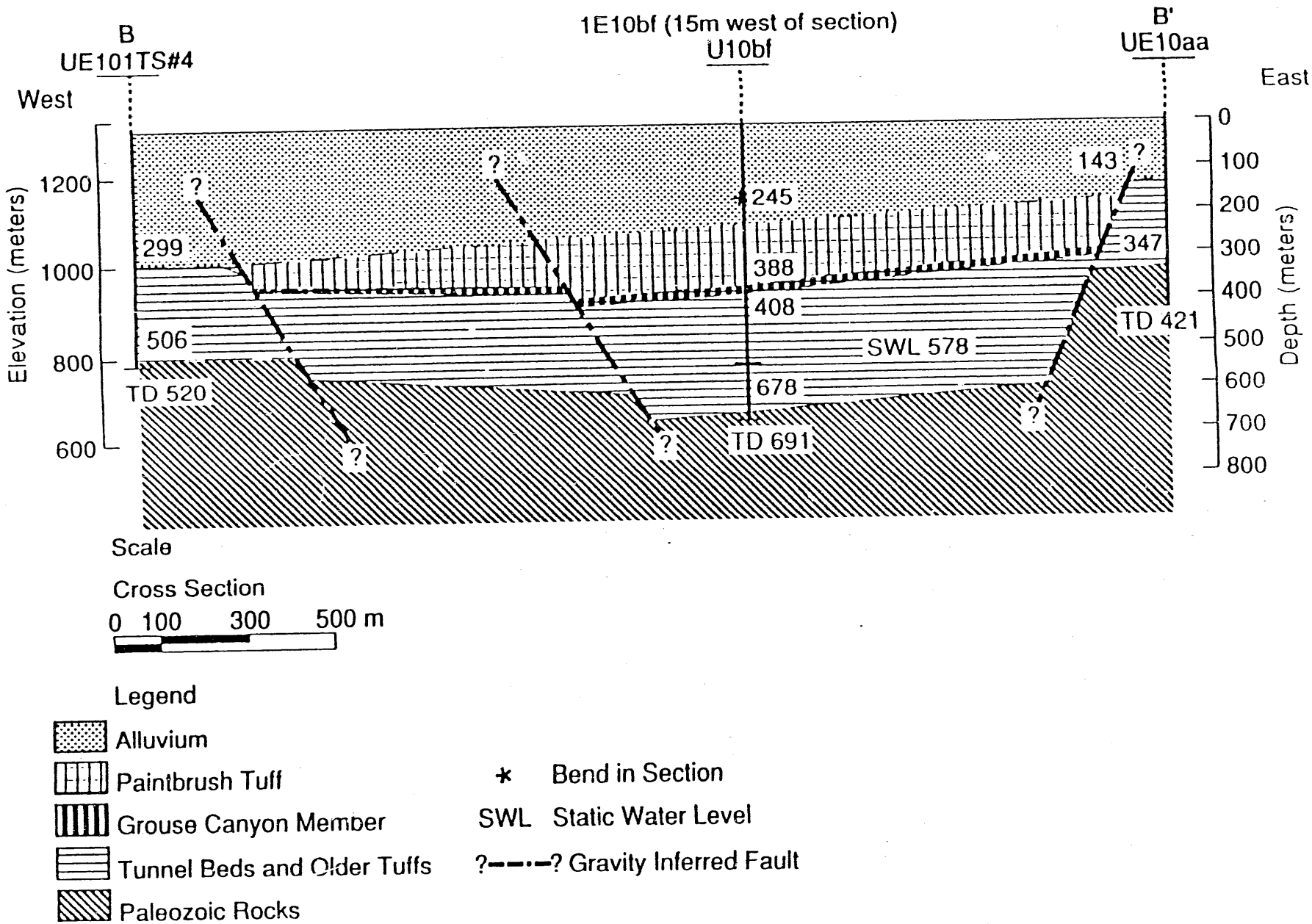

Figure 4. Geologic cross-section along the line BB' shown on the map of Figure 2.

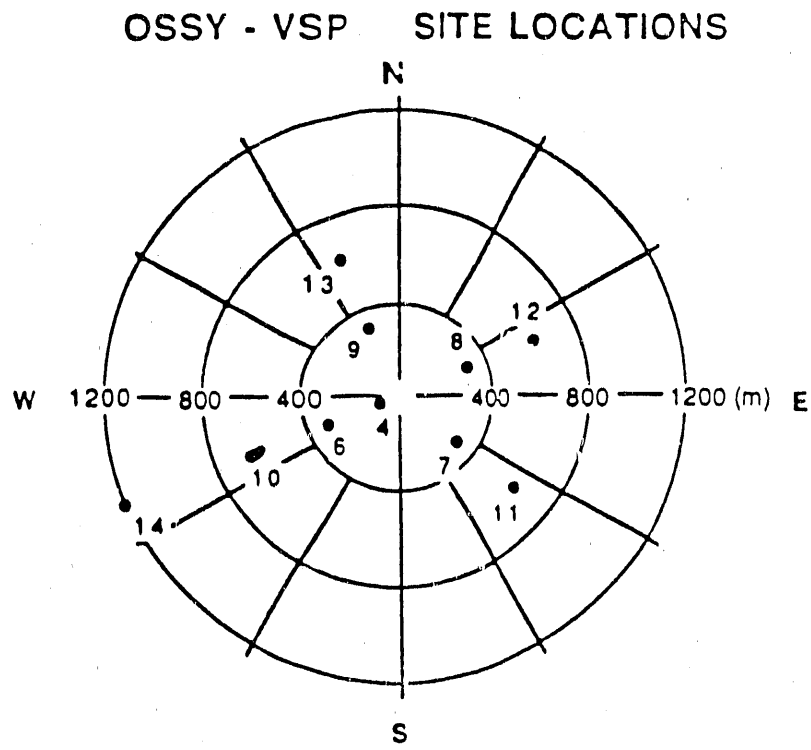

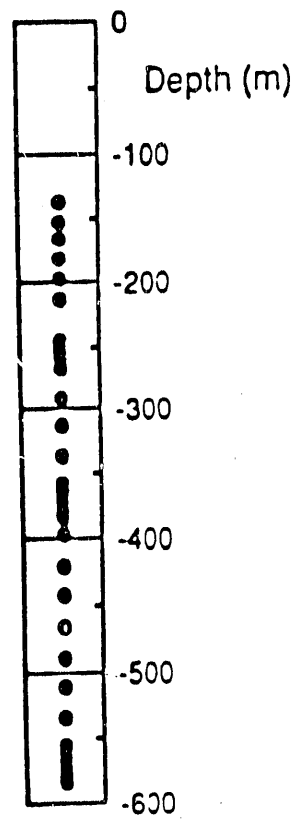

Figure 5. The locations of source and receiver points for the VSP survey.

Table 1. Shot Information for the 1989 OSSY Experiment

Event	Date	OriginTime h:m:s	Depth m	Explosive pounds
OSSY01	Sept 15	20:04:00	578.0	10
OSSY02	Sept 15	20:49:00	569.3	100
OSSY03	Sept 15	21:05:00	537.7	10
OSSY04	Sept 15	21:14:00	529.0	100
OSSY05	Sept 15	21:21:00	497.4	10
OSSY06	Sept 15	21:29:00	488.7	100
OSSY07	Sept 19	19:10:00	448.4	10
OSSY08	Sept 19	19:19:00	439.8	100
OSSY09	Sept 19	19:29:00	408.2	10
OSSY10	Sept 19	19:47:00	399.5	100
OSSY11	Sept 19	19:55:00	367.8	10
OSSY12	Sept 19	20:08:00	359.2	100
OSSY13	Sept 21	17:40:03	328.4	10
OSSY14	Sept 21	18:04:02	319.7	100
OSSY15	Sept 21	18:10:32	288.1	10
OSSY16	Sept 21	18:21:17	279.4	100
OSSY17	Sept 21	18:28:17	247.8	10
OSSY18	Sept 21	18:36:47	239.1	100
OSSY19	Sept 22	15:35:02	199.7	10
OSSY20	Sept 22	15:44:21	191.0	100
OSSY21	Sept 22	15:47:01	159.4	10
OSSY22	Sept 22	15:50:35	150.7	100
OSSY23	Sept 22	16:01:01	119.1	10
OSSY24	Sept 22	16:08:41	110.4	100

arrangement of these recording sites is shown in Figure 6. Note that most of these recording sites are identical to the source sites of the VSP survey shown in Figure 5, thus reversing the paths that that were traversed during the VSP part of the experiment.

The Berkeley portable network which was deployed for this experiment is the same one which has been used to record several nuclear explosions (see Johnson, 1988, for examples). It consists of triggered digital event recorders and three-component force-balanced accelerometers. The sampling rate on each channel is 200 samples per second with 12 bits per sample. Triggering is achieved by comparing short-term and long-term averages. The nominal clipping level for the sensors is about 1 g. While this system has performed quite well during experiments with nuclear explosions, it has a number of limitations which make it less than ideal for the recording of small chemical explosions such as those in the OSSY experiment. This is not suprising because the basic system was designed and constucted almost 20 years ago. One of the problems involves the bandwidth of the system. The anti-alias filters of the system are set at 50 HZ and it is quite likely that the corner frequencies of 10-pound chemical explosions will be at higher frequencies. This means that the full bandwidth of the seismic signal is not captured. Another problem involves the dynamic range. When the level of ground motion is around 1 cm/sec**2 or less it is comparable to the noise level of the sensor, particularly at the lower frequencies. Procedures have been developed for mitigating some of these noise effects in the processing of the data, but the noise can only be partially removed. Another problem resulted from the use of triggered systems to record small events in a noisy environment. This problem appeared in three forms. First, determining a proper level for the trigger level is difficult and often one must rely on a trial and error procedure. During the first series of explosions these trigger levels were set too high and as a result no data were recorded by the Berkeley portable network for the 8 deepest explosions. Second, at the larger ranges the signals from these small chemical explosions were often not large enough compared to the ground and system noise to cause the system to trigger. For this reason no data were obtained from a station at a range of 1200 meters and data for only some of the explosions were obtained from the stations at a range of 625 meters. The third form of the problem showed up at the stations very close to the hole. When working with nuclear explosions there is is rarely a problem with false triggers because there is no human activity in the vicinity of the explosion immediately prior to detonation and the ground motions are large so that trigger levels can be set well above background noise levels. In the case of the OSSY experiment this was not the case. There was considerable activity near the hole while preparing for the detonation of the shots and this often generated enough ground noise to cause false triggers on the stations at closest ranges, particularly because the trigger levels had to be set at low levels in order to capture the small explosions being detonated. In some cases the number of these false triggers was sufficient to fill the recording medium before the explosion was detonated and this led to a loss of data.

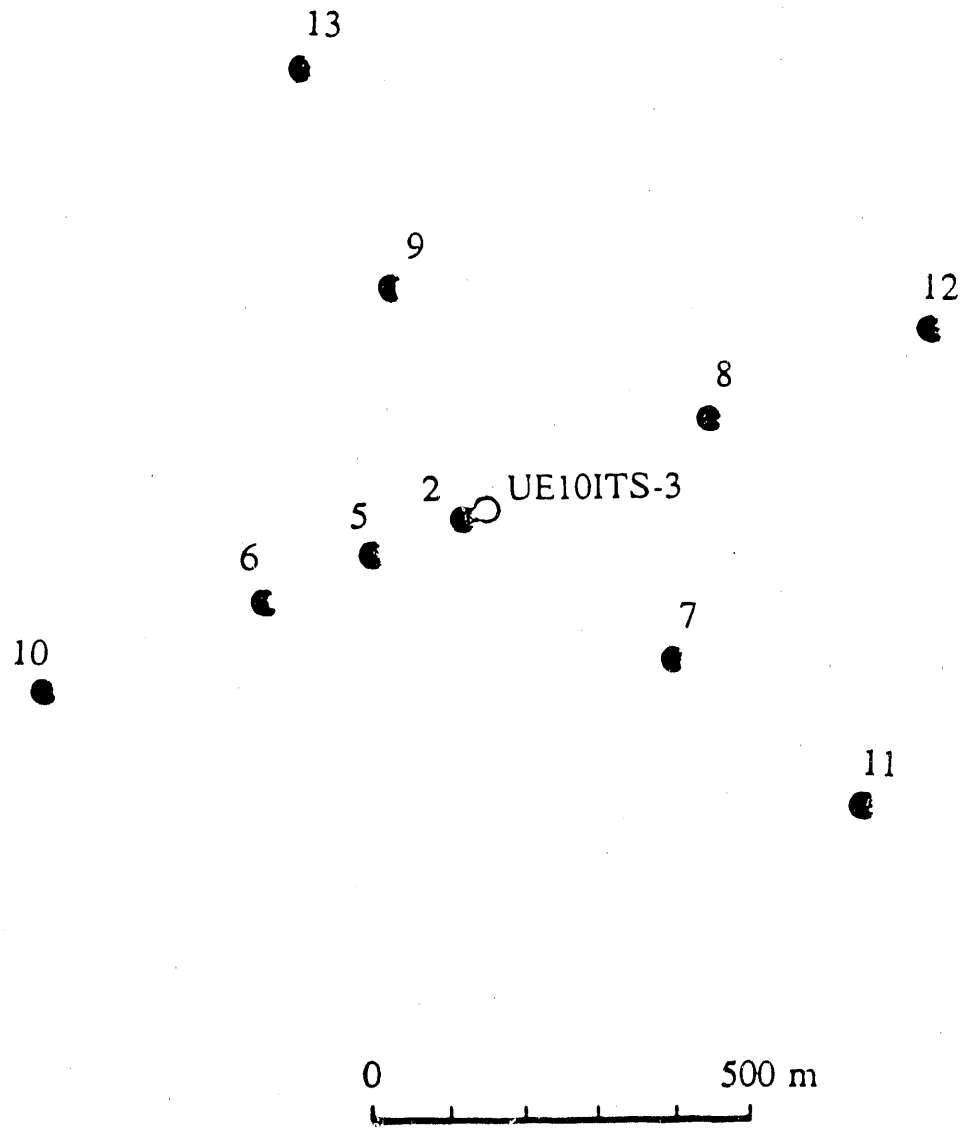

Figure 6. Relative locations of the drilled hole where the explosions were detonated (open circle labeled UE10ITS-3) and the surface sites where seismographs were placed (filled circles with number of site). Most of these receiver sites were identical to the source sites for the VSP survey as shown in Figure 5.

Another part of the experiment was designed to obtain free-field measurements of motions near the explosion sources. Three sets of vertical component gauges were placed in the hole at distances between 1 and 100 meters of various explosions. Both the explosions and the down-hole gauges were grouted in cement. The details of the emplacement procedure can be found in Schaffer (1989). One of the purposes of the down-hole measurements was to provide a check on source properties which were inferred from the surface measurements.

Data analysis

The analysis of the OSSY data can be grouped under three general categories, characterization of the medium, analysis of the free-field data, and analysis of the surface data. The separate tasks associted with these three categories are listed below.

Characterization of the medium

- Analysis of the log data available for the hole
- 3D velocity inversion of both P and S travel time data
- Comparison of VSP data with log data
- Analysis of S-wave splitting to estimate anisotropy
- Estimation of attenuation effects
- Comparison of results with geologic cross sections for the area

Analysis of free-field data

- Analysis of free-field data to examine linearity and yield effects
- Code calculations to aid in interpreting free-field data

Analysis of surface data

- Comparison of surface data with VSP data
- Analysis of surface data to examine yield scaling
- Moment tensor inversion of surface data
- Comparison of surface data with free-field data
- Comparison of results with data from other explosions

The present report will concentrate on results obtained from the third category, the analysis of the surface data. The analysis concerning the characterization of the medium is described primarily in another report (Daley et al., 1990), but some of the results from that part of the study will be used in the present report. The analysis of the free-field data is still in progress and those results will be contained in a later report.

Velocity models

Models of the material properties surrounding the hole were constructed on the basis of the hole log data and the VSP survey. These models were then used to calculate elastodynamic Green functions which were used in turn to extract estimates of the source second-order moment tensors from the seismograms observed at the surface.

The first-arrival times of the VSP data were subjected to a three-dimensional velocity inversion for both P and S waves (Daley et al., 1990). While lateral variations in the velocities were clearly present, the dominant velocity gradients were in the vertical direction and correlated well with changes in lithology. In calculating the Green functions one has a choice between an exact calculation for an approximate one-dimensional velocity model or an approximate calculation for a more accurate three- dimensional velocity model. The former choice has been made for the purposes of this report.

Figures 7 and 8 show two velocity models which have been used in the Green function calculations. Both are based on the data and results contained in the report of Daley et al. (1990). Figure 7 is a one-dimensional model which is a lateral average of the results of the three-dimensional inversion of the VSP travel time data. This method of constructing a velocity model tends to produce the smoothest model which is generally consistent with the data. Thus the model in Figure 7 is quite smooth and has only one sharp feature, a thin low-velocity zone between a depth of 300 and 400 meters, which was included because of a prominent S to P converted phase in the VSP data. Figure 8 was constructed from sonic and density logs that were available for hole UE10ITS3 and from interval velocities calculated from the VSP travel times. This model shows a large amount of structure and shows the alternating highs and lows that are typical of this type of data. It is not known if all of the sharp features of this model are actually real and extend outward from the hole to a significant distance. However, in Figures 7 and 8 we have attempted to bracket the range of possible velocity models which are consistent with the available data, one being a very smooth interpretation and the other being a very irregular interpretation.

Moment tensor inversion

Seismic observations in general contain the combined effect of the source and the effects of wave propagation between source and receiver. In this experiment, since the objective is a characterization of the source, it is necessary to remove the propagation effects. One method of doing this is the procedure known as moment tensor inversion.

So far the moment tensor inversion process has been performed for 13 of the 24 explosions. For some of these events inversions have been performed using both of the velocity models described in the previous section. The preliminary results show that the estimated moment tensor is about the same regardless of which of the two velocity models is used in the inversion process. This is an encouraging result and indicates that the moment tensor estimates are fairly robust with respect to the fine details of the velocity model. However, more tests will have to be performed to substantiate this inference.

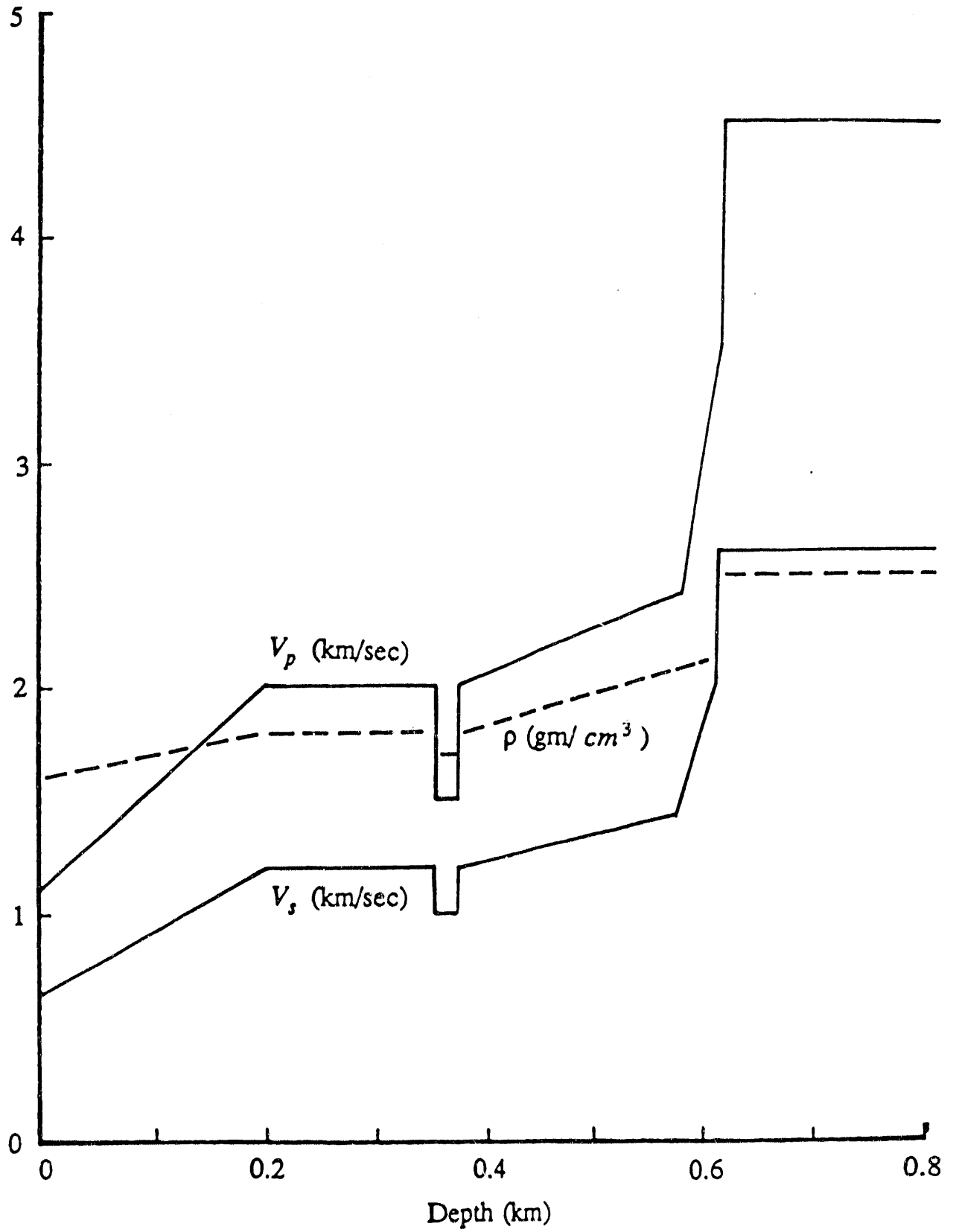

Figure 7. Velocity and density models for the region in the vicinity of hole UE10ITS3. This is an attempt at the smoothest model consistent with the data.

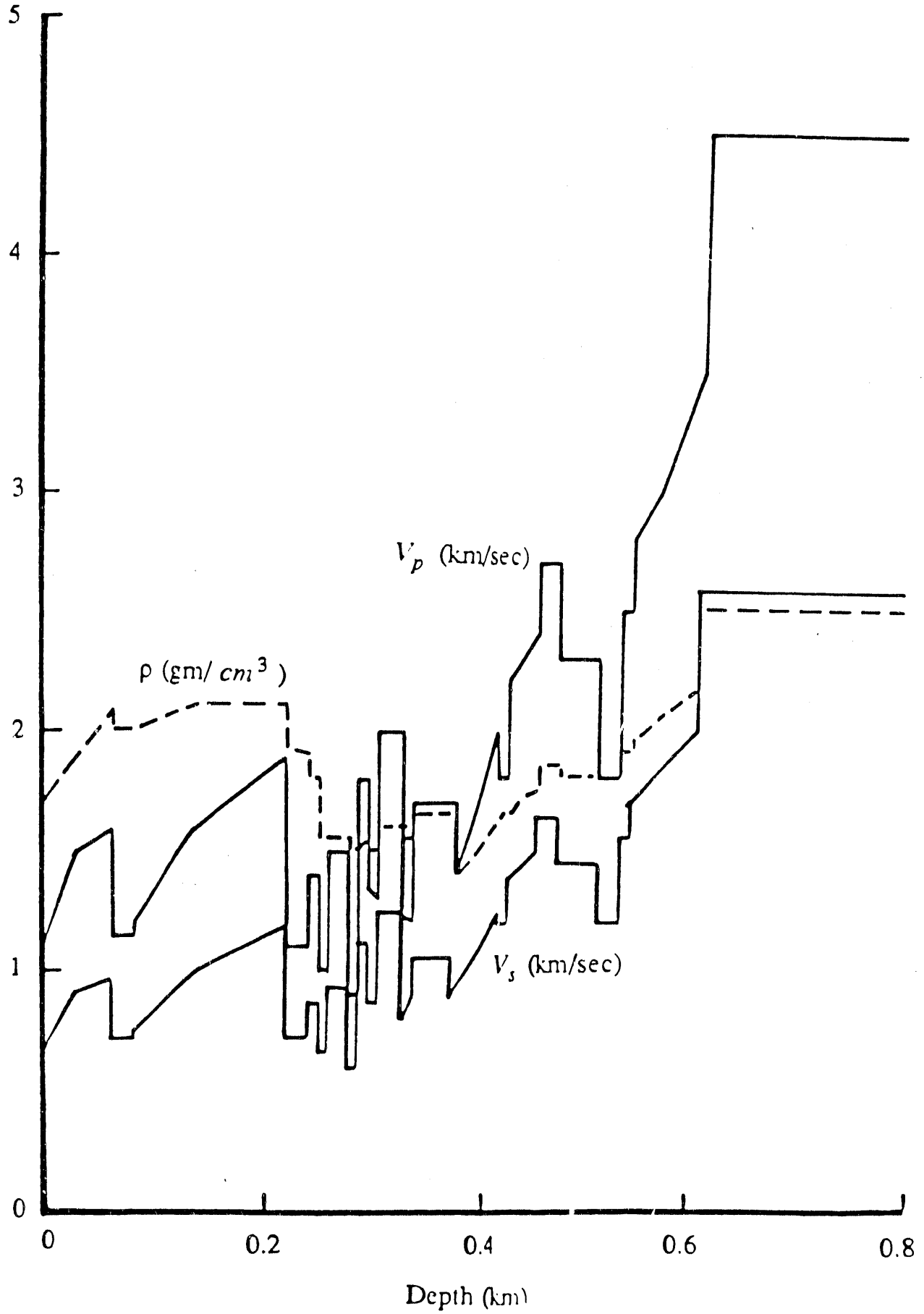

Figure 8. Velocity and density models for the region in the vicinity of hole UE10ITS3. This is an attempt at the most irregular model consistent with the data.

To illustrate the process and the type of results that are obtained, the moment tensor inversion process will be illustrated for one of the explosions. OSSY 21 was a 10 pound explosion at a depth of 159 meters (Table 1). It was recorded at six different surface sites and the distance to these sites along with the maximum recorded accelerations are listed in Table 2. The plots of the data, arranged in order of increasing range and scaled by one over range, are shown in Figures 9, 10, and 11. These data were inverted for estimates of the second-order force-moment tensor at the source point. The inversion was performed in the frequency domain and consisted of doing a singular value decomposition at each frequency. The condition number, taken as the ratio of the maximum to minimum singular value, is shown as a function of frequency in Figure 12. This number is generally less than 10 over the entire frequency range, indicating a good stable solution.

The six elements of the second-order moment rate tensor which were estimated for the explosions OSSY 21 are shown in Figure 13. It is clear in this figure that the moment rate tensor is dominated by the diagonal elements of the tensor, that the time function on these diagonal elements consists primarily of a sharp pulse at the time of the explosion, and that the diagonal elements are quite similar to each other in both the shape and amplitude of this pulse. Thus, this moment rate tensor can be well approximated by a scalar quantity, its trace. Defining the isotropic part of the moment rate tensor as one third its trace, this quantity is displayed in the frequency domain in Figure 14. This spectrum also has a relatively simple form, with a relatively flat low-frequency level extending out to a corner frequency near 50 Hz and a fall off in the spectrum at higher frequencies.

One way of checking the validity of the estimated moment tensor is to compare the data it predicts with the observed data. This has been done in Figure 15 for the station nearest to OSSY 21. In this figure the observed data are shown for the radial, transverse, and vertical components, and below each is the predicted data obtained by convolving the moment tensor estimates of Figure 13 with the Green functions. The correlations are quite good for the entire records. Figure 16 shown similar results for one of the more distant stations. The first parts of the seismograms are well modeled, particularly on the vertical component, but later parts of the records are not modeled nearly so well, with the transverse component showing very little correlation.

One of the objectives of this study was to analyze the effects of source size, source depth, and source medium upon the coupling of explosive sources. Figure 17 is an attempt to present some of these data. The low frequency level of the isotropic part of the estimated moment tensor has been scaled by the yield of the explosion W and plotted against the scaled depth of the explosion. The depth has been scaled by the yield to the one third power. Shown on this plot are the results from preliminary moment estimates for a number of the OSSY shots, including yields of both 10 and 100 pounds. Also shown on this figure are similar results from a series of chemical explosions in the Kaiser Quarry near Menlo Park, California (McEvilly and Johnson, 1989). These explosions had yields between 300 and 1000 pounds and burial depths between 10 and 217 meters. One of the reasons for including the Kaiser Quarry data

Table 2 Maximum Accelerations from Event OSSY21

Station	Azimuth deg E of N	Range m	Distance m	max R cm/sec**2	max T cm/sec**2	max Z cm/sec**2
UCB02	248	21.9	160.9	2.1	2.7	10.4
UCB05	248	157.5	224.1	4.2	4.2	5.1
UCB06	248	314.5	352.6	1.1	2.3	1.6
UCB07	128	314.5	352.6	1.5	1.5	1.8
UCB08	68	314.5	352.6	2.2	1.1	2.0
UCB09	338	314.5	352.6	1.2	1.0	1.7
UCB10	248	626.5	646.5	0.2	0.4	0.2

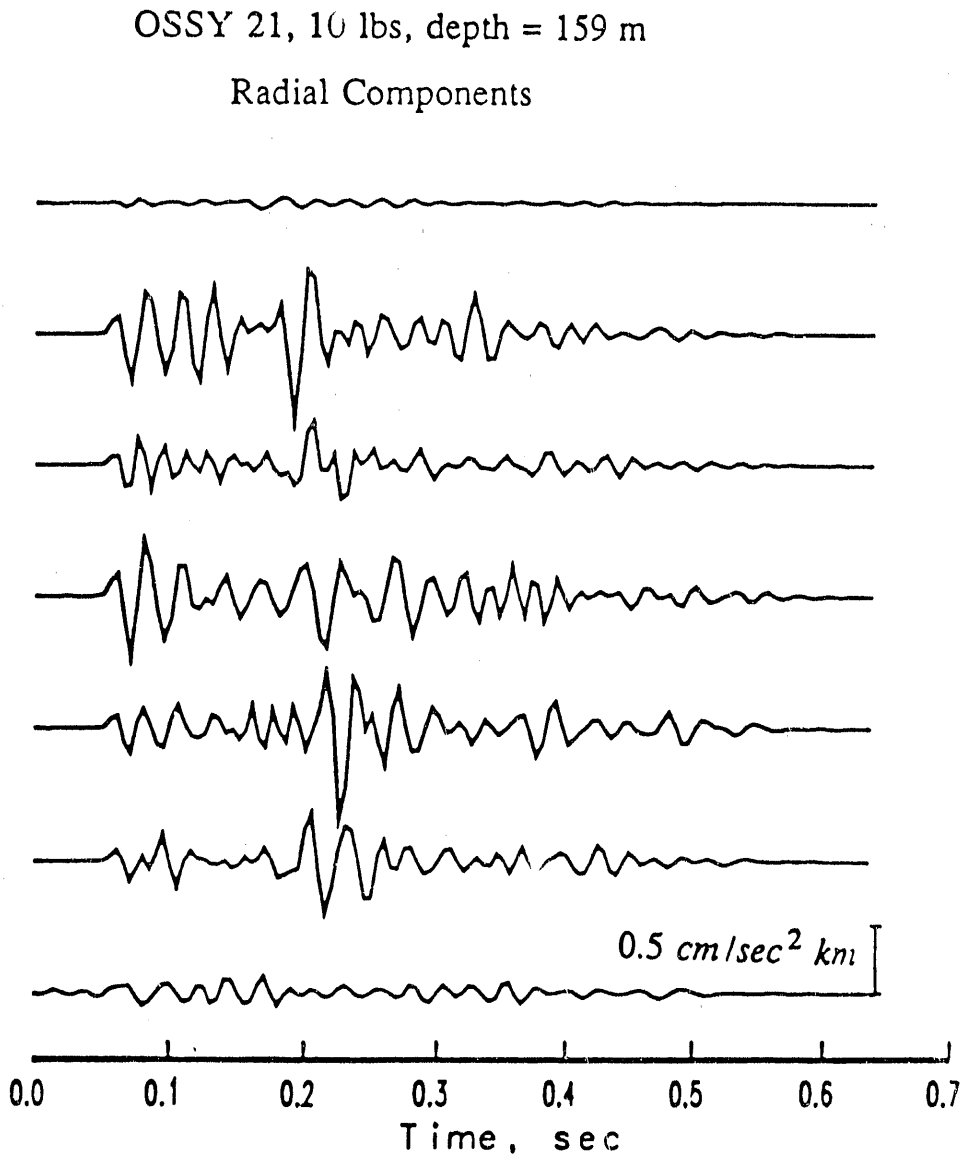

Figure 9. Radial accelerations observed at the surface for the explosion OSSY 21. The data are scaled by inverse range and are in same order as in Table 2.

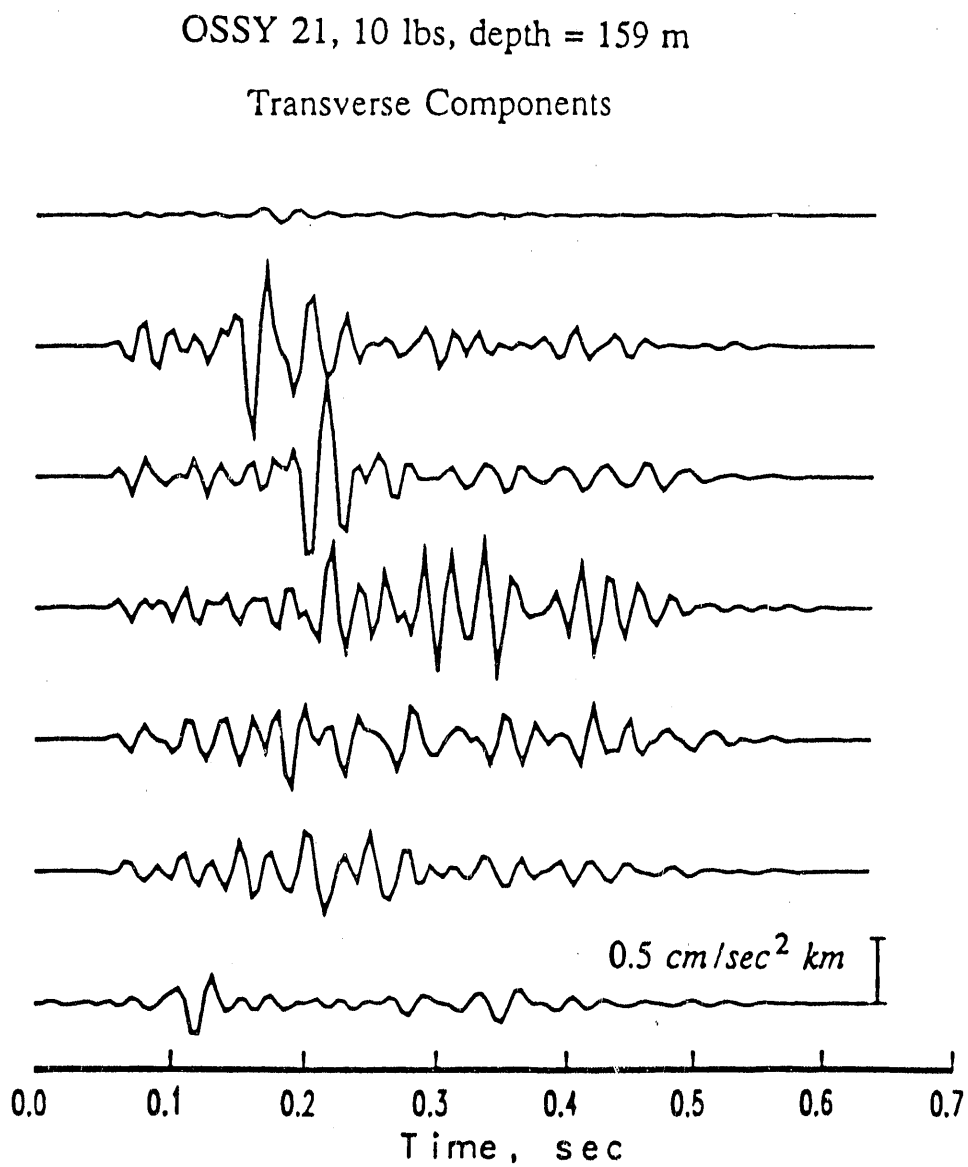

Figure 10. Transverse accelerations observed at the surface for the explosion OSSY 21. The data are scaled by inverse range and are in same order as in Table 2.

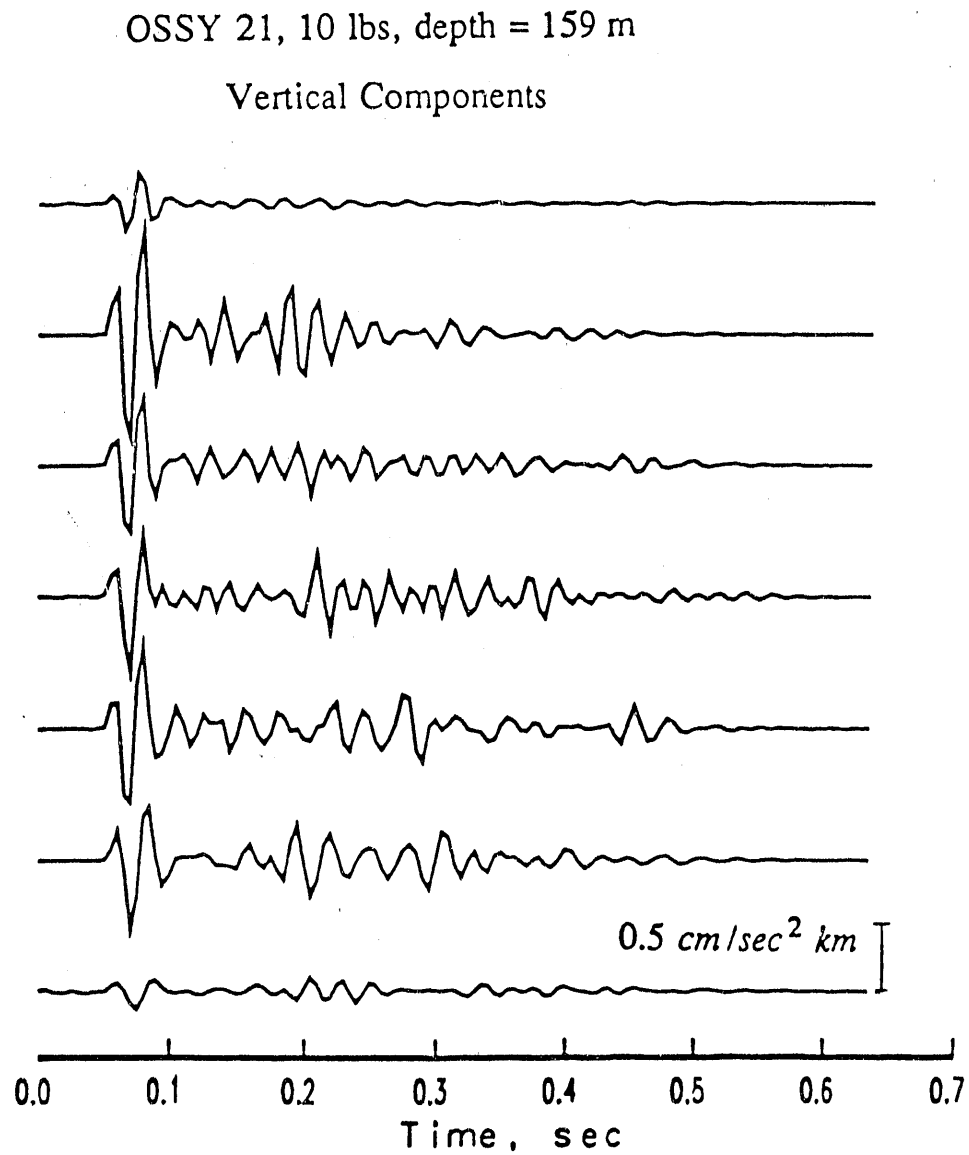

Figure 11. Vertical accelerations observed at the surface for the explosion OSSY 21. The data are scaled by inverse range and are in same order as in Table 2.

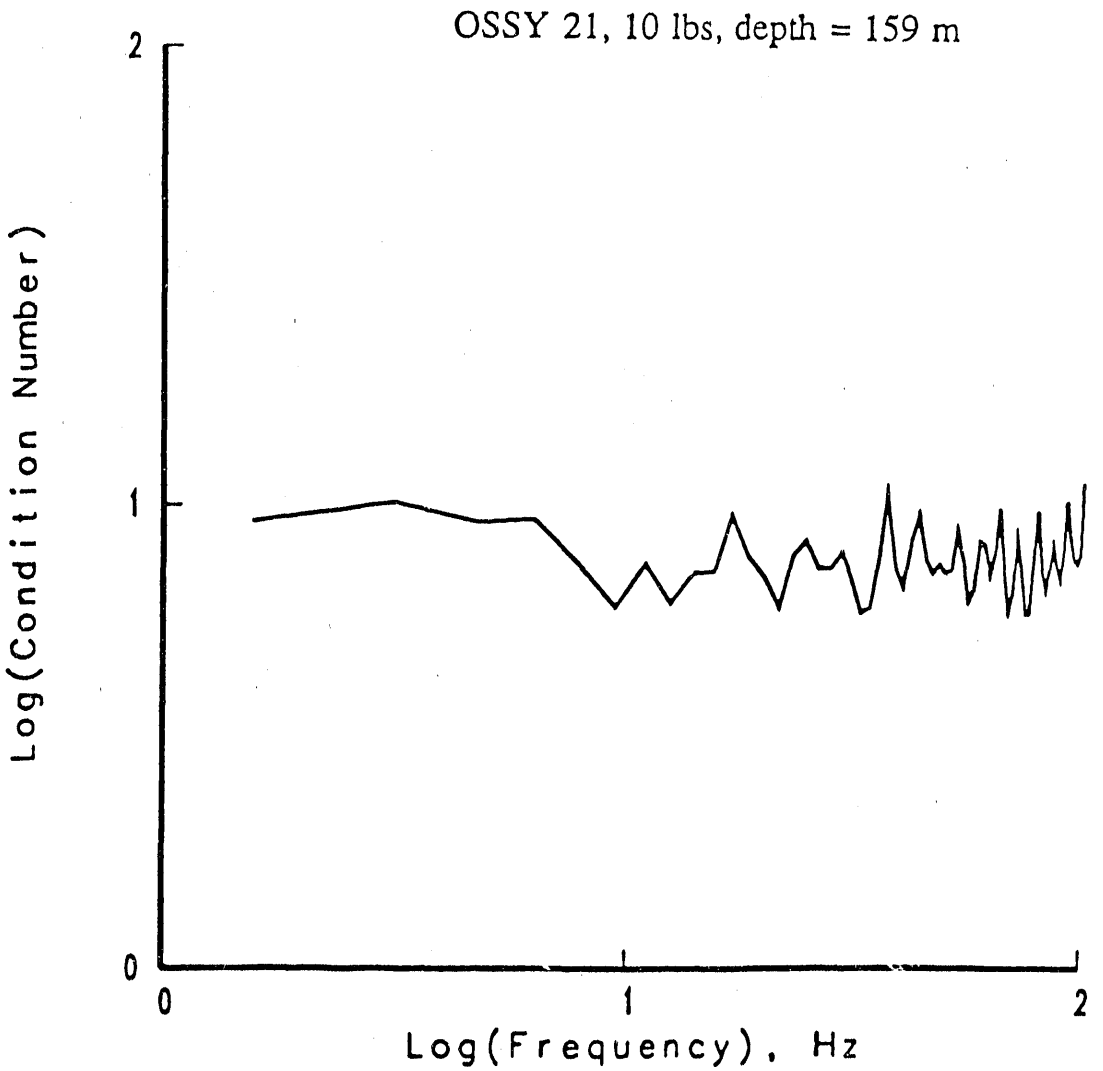

Figure 12. The condition number for the moment tensor inversion of OSSY 21.

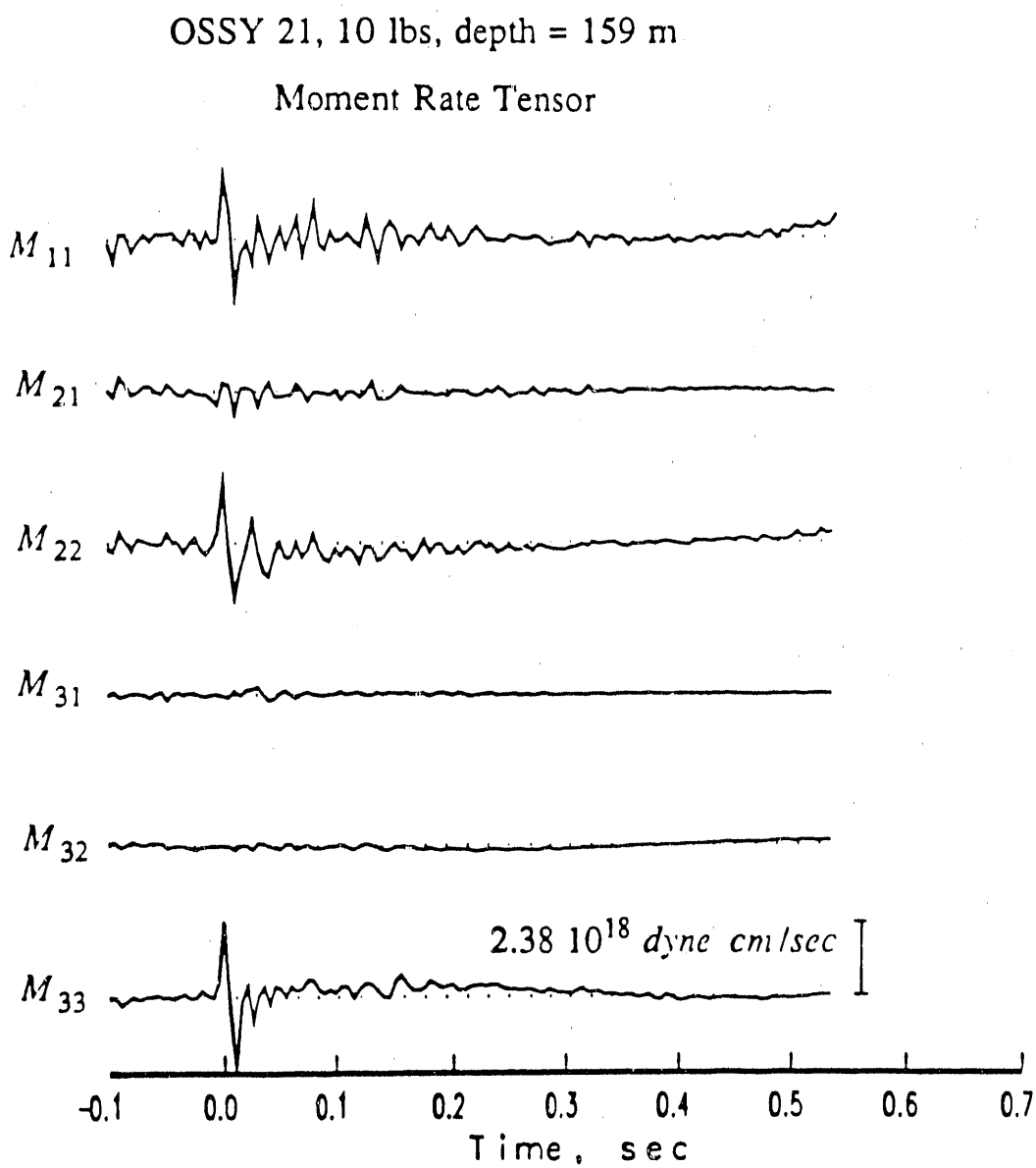

Figure 13. The six independent elements of the second-order moment rate tensor which were estimated for the explosion OSSY 21.

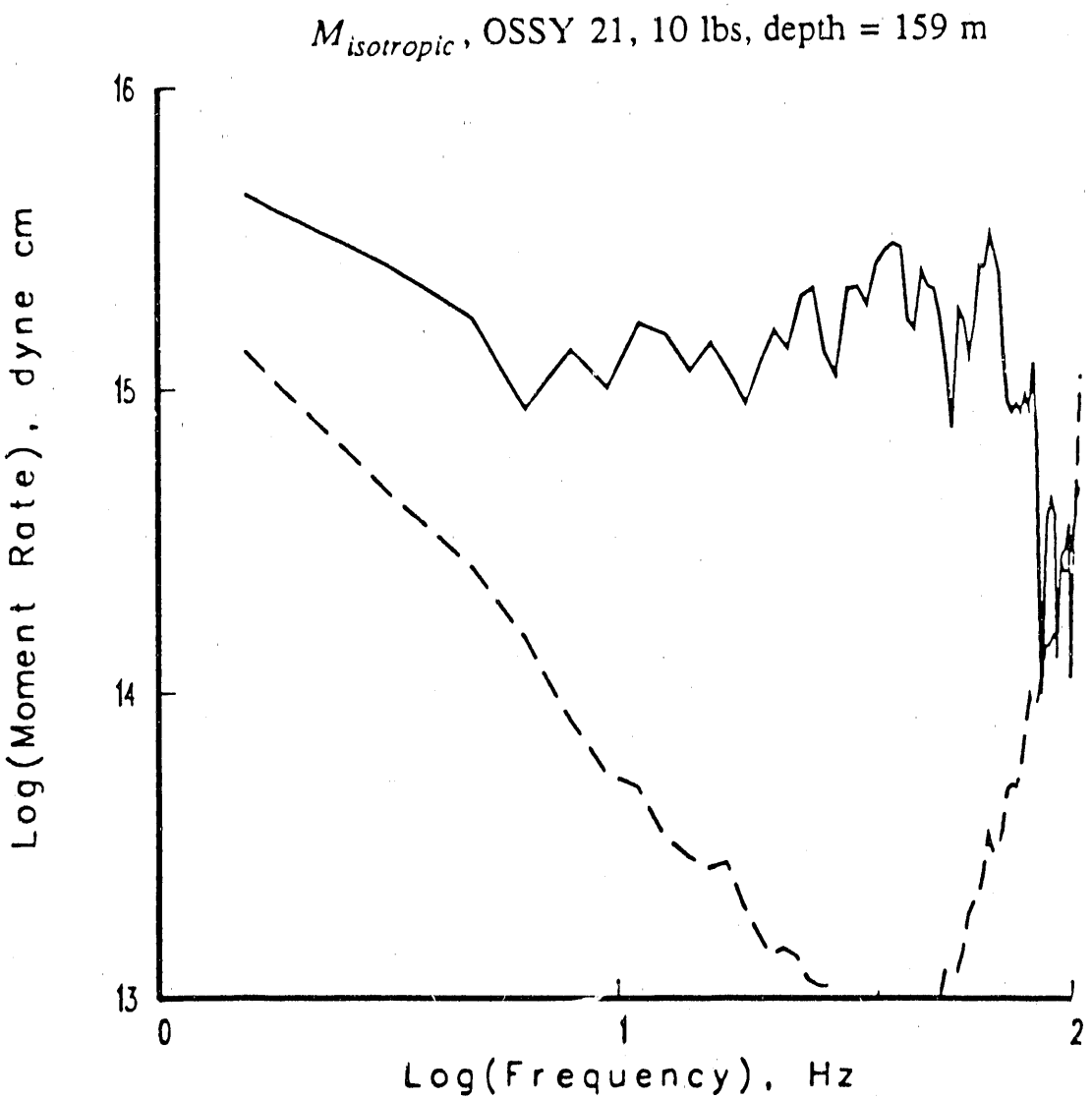

Figure 14. The spectrum of the isotropic part of the moment-rate tensor shown in Figure 13. The dashed line is the estimated standard error of the spectrum.

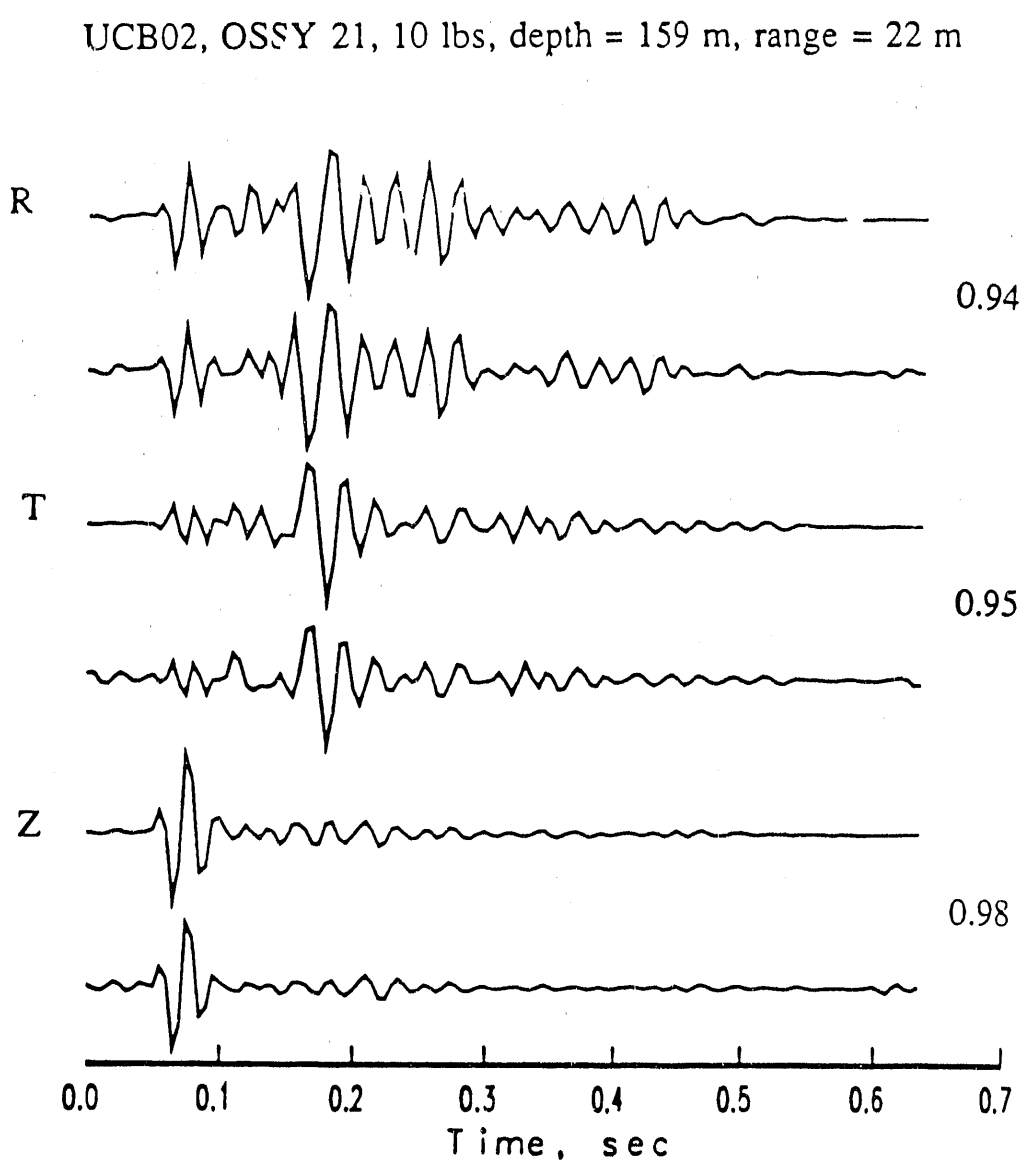

Figure 15. Comparison of observed and predicted data at station UCB 2 for the explosion OSSY 21. The traces labeled R, T, and Z are the observed accelerations in the radial, transverse, and vertical directions. Below each is shown the results of convolving the moment tensor estimates of Figure 13 with the calculated Green functions for the velocity model of Figure 7. The numbers on the right are the correlation

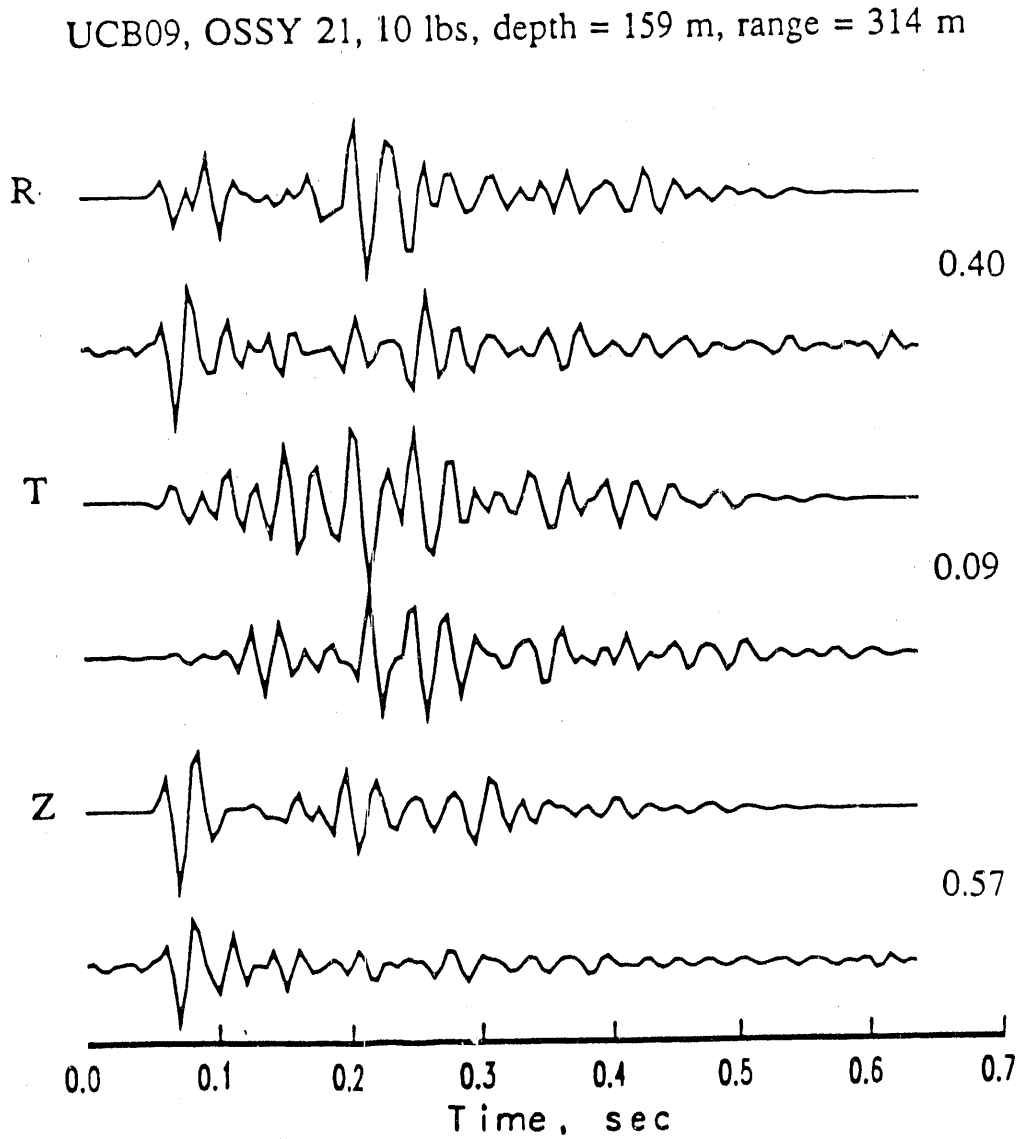

Figure 16. Comparison of observed and predicted data at station UCB 9 for the explosion OSSY 21. The traces labeled R, T, and Z are the observed accelerations in the radial, transverse, and vertical directions. Below each is shown the results of convolving the moment tensor estimates of Figure 13 with the calculated Green functions for the velocity model of Figure 7. The numbers on the right are the correlation

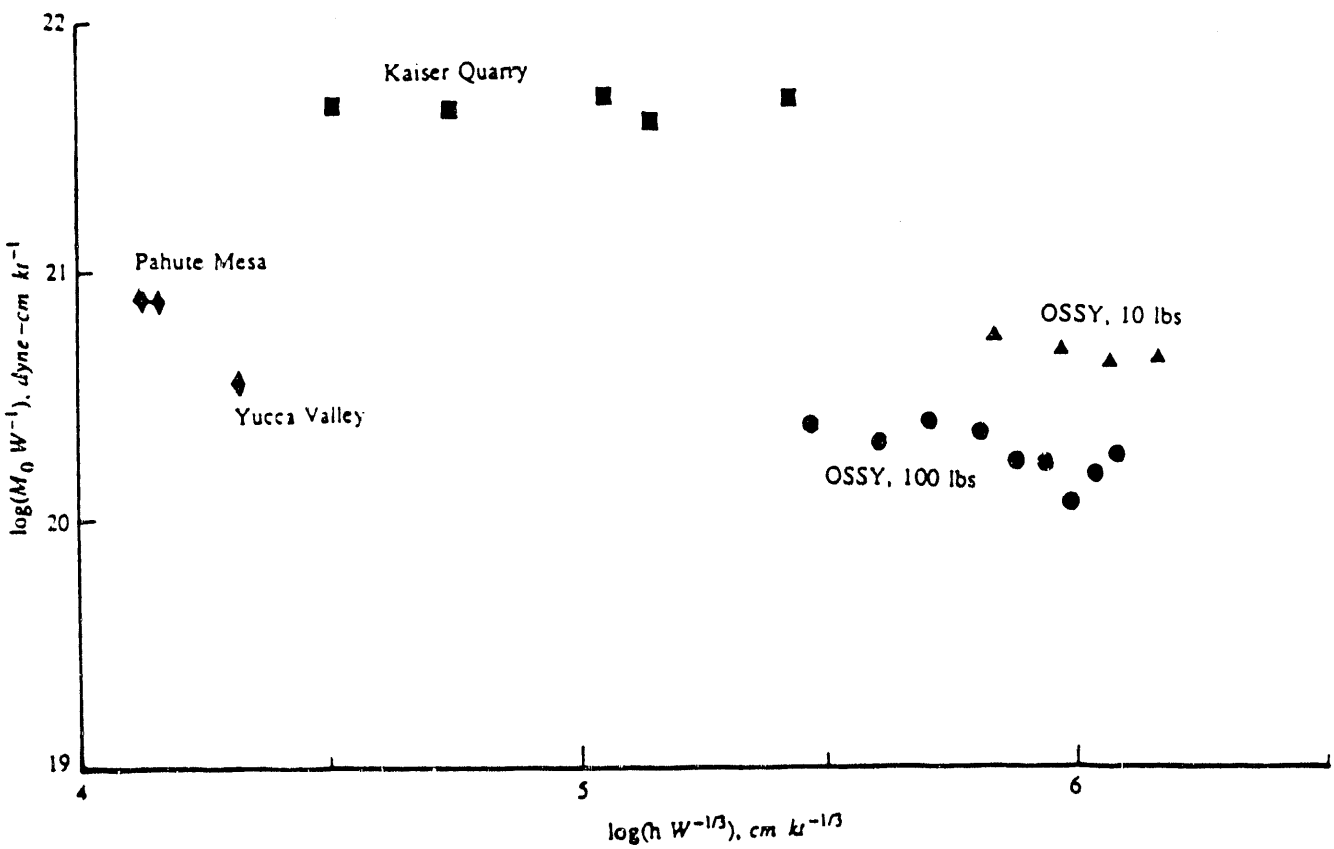

Figure 17. Scaled values of the low-frequency level of the isotropic moment tensor versus scaled depths for a variety of different explosions.

is that the source medium was limestone, which is considerably different from the alluvium and tuff which were the source media for the OSSY events. The three remaining data points in Figure 17 are all nuclear explosions. The two Pahute Mesa events are Harzer and Chancellor which had depths of 637 meters and 625 meters, respectively (Johnson, 1988). The Yucca Valley event is Coalora, which had a depth of 278 meters. The yields of all three of these events are not announced, and so estimates of the yields were obtained from magnitudes determined at Berkeley. It is important to point out that all of the events shown in Figure 17 were subjected to the same moment tensor inversion procedure.

While the axes of Figure 17 display the scaled dependence upon source size and source depth, it is likely that the effects of source medium are also affecting the results that are plotted here. The source medium for the Kaiser Quarry experiment had considerably higher density and velocities than for the NTS events, and the moment tensors estimated for these events fall well above corresponding estimates for the NTS events. This suggests that the isotropic moment tensor is a function of not only the size of the explosion but also of the source medium. Indeed, if one considers the definition of the moment tensor, this is the case. Thus the question arises whether plots such as Figure 17 are the best way of displaying the data so as to isolate the separate effects of source size, source depth, and source medium. This leads to a consideration of various ways of characterizing the size of a seismic event and of how these characterizations depend upon the source medium.

Measures of Source Size

A fairly general description of an indigenous seismic source which is localized in space is given by the first-order moment tensor M, whose elements can be defined as

$$M_{ij}(t) = \int_V f_i(t) x_j \, dV(\mathbf{x}) \tag{1}$$

where f is an equivalent body force and V is the source volume (see Stump and Johnson, 1977). While $\mathbf{M}(t)$ is a second rank tensor, in many situations it is sufficient to consider some scalar norm of $\mathbf{M}(t)$. For instance, in the case of earthquakes which can be approximated by a simple shear dislocation, such a norm is given by the scalar shear moment which is obtained from the deviatoric part of the moment tensor and has the definition

$$M_o(t) = \mu \bar{d}(t) A \tag{2}$$

where μ is the shear modulus, $\bar{d}$ the average dislocation, and A the area of the dislocation surface. Here we have defined the scalar moment as a function of time t. Often this if further simplified to include only the static value of the dislocation and then we have

$$M_o = M_o(\infty) = \mu \bar{d}(\infty) A \tag{3}$$

In the case of explosions, it is convenient to consider the isotropic moment which is obtained from the trace of the moment tensor and defined by

$$M_I(t) = \frac{1}{3}\, trace\,[\mathbf{M}(t)] \tag{4}$$

Note that these definitions for scalar moments of earthquakes and explosions are complementary, in that the isotropic moment of an idealized earthquake is zero and the shear moment of an idealized explosion is zero.

Much of the early work on explosions is formulated in terms of the reduced displacement potential $\Psi(t)$ (Sharpe, 1942). This is a convenient scalar quantity because for a spherically symmetric source the displacement u at a distance r from the source is given simply by

$$\mathbf{u}(r,t) = -\nabla \frac{\Psi(t - r/\alpha)}{r} \tag{5}$$

where α is the velocity of compressional waves in the medium. The reduced displacement potential is simply related to the isotropic moment as follows

$$\Psi(t) = \frac{M_I(t)}{4\pi\rho\alpha^2} \tag{6}$$

It should be pointed out here that the concept of a reduced displacement potential is developed for a homogeneous isotropic medium, and in that case there is no ambiguity in choosing the material parameters that appear in equations (5) and (6). However, if one wants to extend this concept to inhomogeneous materials, then the choice of these parameters becomes more problematical. For instance, since the reduced displacement potential is used to relate the pressure pulse on the interior of a cavity at the source to the displacement at the receiver, it is not obvious in equation (6) whether the ρ and α should have values appropriate for the source point, the receiver point, or some average of the two. We will provide an answer to this question below.

In recent years there have been a number of attempts to produce measures of seismic source strength that are not so dependent on the material parameters that are assumed for the source region. For instance, Heaton and Heaton (1989) consider static deformations produced by a source near a discontinuity in material properties and conclude that the potency introduced by Ben-Menahem and Singh (1981) is a better scalar measure of source size that the scalar shear moment. Potency can be defined by

$$P = \frac{M_o(\infty)}{\rho_s \beta_s^2} \tag{7}$$

where ρ_s and β_s are the density and shear velocity, respectively, at the source point. However, Ruff (1990) considers the radiation of far field body waves from seismic source and suggests that a measure of source size that is even better than potency in terms of independence of material properties in the source region is the seismic reaction, defined by

$$R = \frac{M_o(\infty)}{\rho_s \beta_s} \tag{8}$$

Let us consider another approach to the problem of finding a convenient measure of source strength. Consider a spherically symmetric source where the region in the vicinity of the source is homogeneous and has density ρ_s and compressional velocity α_s. The moment tensor for such a source is completely defined by its isotropic part, and so we define the seismic source strength by

$$S(t) = \frac{\dot{M}_I(t)}{\sqrt{4\pi\rho_s\alpha_s^5}} \tag{9}$$

where $\dot{M}_I$ denotes the derivative with respect to time of M_I. The reasons for choosing such a normalization in terms of material properties is clear when one considers the energy of the source that goes into radiated elastic waves. Consider the far field compressional waves that are generated by this source and calculate the total energy flux through any surface that surrounds the source. Then using the expressions given by Aki and Richards (1980, p. 116 and 424) this total radiated elastic energy is given by

$$E = \int_0^\infty \dot{S}(t)^2\, dt \tag{10}$$

Thus we see that the seismic source strength defined by equation 9 leads to a measure of radiated elastic energy that is independent of material properties at the source. Note that if we let $S(f)$ be the Fourier transform of $S(t)$ and use Parseval's relation, then we also have

$$E = 4\pi^2 \int_{-\infty}^{\infty} S(f)S(f)^*\, f^2\, df \tag{11}$$

In analogy with equation (3), the long-time or long-period level of the source strength can be defined by

$$S_o = S(f=0) = \int_0^\infty S(t)\, dt = \frac{M_I(\infty)}{\sqrt{4\pi\rho_s\alpha_s^5}} \tag{12}$$

It is clear that S_o is the low-frequency spectral level of the source strength as defined in equation (9).

In the case where the material properties near the source and receiver are different the usual treatment of the reduced displacement potential must also be modified. Let us define a scaled version of the reduced displacement potential by

$$\Psi_r(t) = \sqrt{\frac{\rho_s\alpha_r}{\rho_r\alpha_s}}\,\Psi(t) \tag{13}$$

where the subscript r refers to material properties at the receiver site. Using Ψ_r in place of Ψ in equation (5) will then properly scale the far-field term of the displacement calculated from this expression. Equation (6) must also be modified and we now have

$$\Psi_r(t) = \sqrt{\frac{\alpha_r}{4\pi\rho_r}}\,\frac{M_I(t)}{\sqrt{4\pi\rho_s\alpha_s^5}} \tag{14}$$

The utility of the measures of source strength introduced in equations (9) and (12) can be demonstrated with a simple example. For the Sharpe model of an explosion consisting of a step in pressure P_o on the interior of a spherical cavity of radius r_o the reduced displacement potential in the frequency domain is

$$\Psi(f) = \frac{\Psi_\infty}{\sqrt{1-2(1-\eta)(f/f_c)^2+(f/f_c)^4}} \tag{15}$$

where

$$\Psi_\infty = \frac{r_o^3}{2\rho\alpha^2\eta} P_o \tag{16}$$

$$f_c = \frac{\sqrt{2\eta}\alpha}{2\pi r_o} \tag{17}$$

$$\eta = 2\frac{\beta^2}{\alpha^2} \tag{18}$$

Then the source strength in the frequency domain is

$$S(f) = \frac{-i\,2\pi f S_o}{\sqrt{1-2(1-\eta)(f/f_c)^2+(f/f_c)^4}} \tag{19}$$

Then evaluating the integral in equation 11 the radiated elastic energy becomes

$$E = \frac{2\pi^3 f_c^3 S_o^2}{\sqrt{2\eta}} \tag{20}$$

Now S_o is just the low-frequency level of the source strength spectrum and f_c is simply related to the corner frequency of that same spectrum. For the Sharpe model the amount of peaking of the spectrum above its low-frequency level is controlled by the parameter η so in principle this could also be determined from the spectrum. Thus the spectrum of the seismic source strength as defined in equation (9) contains all of the information required to estimate the energy which the source has put into radiated elastic energy.

Having developed an alternative expression for the size of a seismic source, this can be tested with the same data shown in Figure 17. These same data are plotted in Figure 18 with the scaled values of the low frequency levels of the seismic source strength (equation 12) substituted for the scaled isotropic moment tensor. It is clear that, whereas there is a significant separation between the Kaiser Quarry data and the OSSY data in Figure 17, this separation has been greatly reduced in Figure 18 where the two data sets appear to lie along the same general trend.

Conclusions

The analysis of these data is still in progress so conclusions given at this time must be considered preliminary. Furthermore, several groups are analyzing different parts of the experiment and the results from these different parts have not yet been completely coordinated. However, the following general conclusions seem warranted

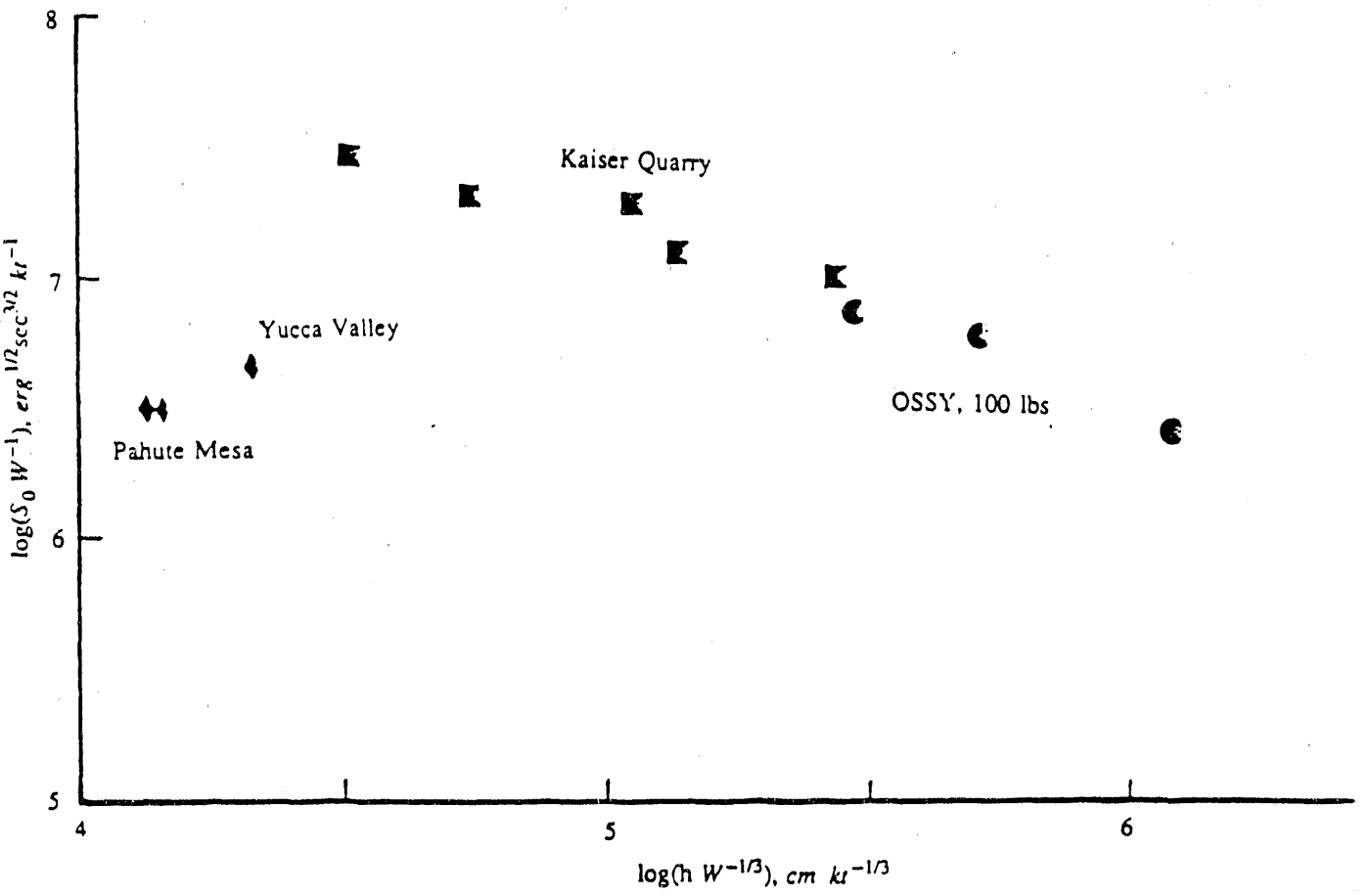

Figure 18. Scaled values of the low-frequency level of the seismic source strength versus scaled depths for a variety of different explosions.

at the present time:

1) In the course of designing and performing this experiment it was quite evident that, in terms of both flexibility of design and ability to control parameters, small chemical explosions have many advantages over nuclear explosions. Most of the important features of the OSSY experiment could not have been achieved with nuclear explosions.

2) Chemical explosions of this type provide a convenient means of expanding the available data base with respect to such parameters as source size, source depth, and source medium.

3) During this experiment considerable effort was devoted to the measurement of material properties in the vicinity of the explosions. Thus the velocity models used in the moment tensor inversions were better constrained than in most of our previous studies of nuclear explosions at NTS. These velocity models have turned out to be rather complicated. However, the tests conducted so far indicate that the estimated moment tensors are quite robust with respect to fine details of the velocity models.

4) In examining scaling relationships between source size and source depth, care must be taken to use a measure of source size that is independent of the source medium. A measure of seismic source strength based on energy considerations has been developed which appears to have this property.

5) The surface motions measured by UC Berkeley during this experiment were obtained with a portable seismographic network which was developed for the study of nuclear explosions at NTS. This recording system is quite old and has certain deficiencies in both sensitivity and bandwidth which become much more serious when studying small chemical explosions than when studying the larger nuclear explosions.

Continuing Work

The OSSY experiment generated a large amount of data and some of these data were quite different from what had been produced by similar experiments in the past. This meant that it has been necessary to develop some new methods of analysis. What has been completed so far is an initial pass through just about all of the analysis procedures which are contemplated. These analysis procedures all seem to be producing good results and there seems to be no doubt that the OSSY experiment was quite successful. However, in order to take advantage of all of the many different types of information which were developed in the process of doing the initial analysis, it seems worth while to make a second pass through all of the analysis and in this way arrive at the final results of the experiment. Given the large amount of data involved and the time required by some of the analysis procedures, care is being taken in designing this second analysis run in such a way that it does not have to be repeated a third time.

It is desirable that the analysis of velocity models be completed before beginning the second run of the moment tensor inversions. While much of this has been

completed for the P and S velocities, the attenuation properties of both of these wave types still requires further analysis. Once estimates of these attenuation properties are available, it should be straightforward to generate the appropriate Green functions and perform the moment tensor inversions.

References

Aki, K., P. G. Richards, Quantitative Seismology, Vol. I, W. H. Freeman, San Francisco, 557 pp, 1980.

Ben-Menahem, A., S. J. Singh, Seismic Waves and Sources, Springer-Verlag, New York, 1108 pp, 1981.

Daley, T. M., T. V. McEvilly, A. Michelini, VSP site characterization at NTS - Summary report, August 1990,

Heaton, T. H., R. E. Hutton, Static deformations from point forces and force couples located in welded elastic Poissonian halfspaces: implications for seismic moment tensors, Bull. Seism. Soc. Am., 79, 813-841, 1989.

Johnson, L. R., Source characteristics of two underground nuclear explosions, Geophys. J., 95, 15-30, 1988.

McEvilly, T. V., L. R. Johnson, Regional studies of broadband data, Report GL-TR-89-0224, Geophysics Laboratory, Hanscom Air Force Base, 57 pp, August 1989.

Ruff, L., B. Tichelaar, Is seismic moment the best measure of earthquake size?, Seismol. Res. Let., 61, p27, 1990.

Schaffer, Tom, OSSY preliminary test results, X-Ray Diagnostics Group, Memo to Jim Pastrone, October 10, 1989.

Stump, B. W., L. R. Johnson, The determination of source properties by the linear inversion of seismograms, Bull. Seism. Soc. Am., 67, 1489-1502, 1977.

END

DATE FILMED

01 / 15 / 91